Biogeosciences Discuss., doi:10.5194/bg-2017-17, 2017
Manuscript under review for journal Biogeosciences
Discussion started: 9 February 2017

Biogeosciences Discussions Open Access EGU

Simulating precipitation decline under a Mediterranean deciduous Oak forest: effects on isoprene seasonal emissions and predictions under climatic scenarios.

Anne-Cyrielle Genard-Zielinski[1,2], Christophe Boissard[2], Elena Ormeño[1], Juliette Lathière[2], Ilja M. Reiter[3], Henri Wortham[4], Jean-Philippe Orts[1], Brice Temine-Roussel[4], Bertrand Guenet[2], Svenja Bartsch[2], Thierry Gauquelin[1] and Catherine Fernandez[1]

[1]Institut Méditerranéen de Biodiversité et d'Ecologie marine et continental, Aix Marseille Université-CNRS-IRD-Univ. Avignon, Marseille, 13331CEDEX 3, France

[2]Laboratoire des Sciences du Climat et de l'Environnement, LSCE/IPSL, CEA-CNRS-UVSQ, Université Paris-Saclay, Gif-sur-Yvette, 91191, France

[3]Fédération de Recherche 'Ecosystèmes Continentaux et Risques Environnementaux', CNRS FR 3098 ECCOREV, Technopôle de l'environnement Arbois-Méditerranée, Aix-en-Provence, 13545, France

[4] Laboratoire de Chimie de l'Environnement, Aix Marseille Université, CNRS, UMR 7376, Marseille, 13331, France

Correspondence to : Christophe Boissard, (christophe.boissard@lsce.ipsl.fr).

Abstract. Seasonal variations of *Q. pubescens* physiology and isoprene emission rates (ER) were studied from June 2012 to June 2013 at the O_3HP site (French Mediterranean) under natural (ND) and amplified (+30%, AD) drought. While AD significantly reduced the stomatal conductance to water vapour over the season excepting August, it did not significantly limit CO_2 net assimilation, which was the lowest in summer. ER followed a significant seasonal pattern, whatever the drought intensity, with mean ER maxima of 78.5 and 104.8 µgC g_{DM}^{-1} h^{-1} in July (ND) and August (AD) respectively. Isoprene emission factor increased significantly by a factor of 2 in August and September under AD (137.8 and 74.3 µgC g_{DM}^{-1} h^{-1}) compared to ND (75.3 and 40.21 µgC g_{DM}^{-1} h^{-1}), but no changes occurred on ER. An isoprene algorithm (*G*14) was developed using an optimised artificial neural network trained on our experimental dataset (ER + O_3HP climatic and edaphic parameters cumulated over 0 to 21 days before measurements). *G*14 assessed more than 80% of the observed ER seasonal variations, whatever the drought intensity. In contrast, ER was poorly assessed under water stress by MEGAN empirical isoprene model, in particular under AD. Soil water (SW) content was the dominant parameter to account for the observed ER variations, regardless the water stress treatment. ER was more sensitive to higher frequency environmental changes under AD (0 to -7 days) compared to ND (7 days). Using IPCC RCP2.6 and RCP8.5 climate scenarios, SW and temperature calculated by the ORCHIDEE land surface model, and *G*14, an annual 3 fold ER relative increase was found between present (2000-2010) and future (2090-2100) for RCP8.5 scenario compared to a 70% increase for RCP2.6. Future ER

Biogeosciences Discuss., doi:10.5194/bg-2017-17, 2017
Manuscript under review for journal Biogeosciences
Discussion started: 9 February 2017

remained mainly sensitive to SW (both scenarios) and became dependent to higher frequency environmental changes under RCP8.5.

1. Introduction

A large number of Mediterranean deciduous and evergreen tree species produce and release isoprene (2-methyl-1,3-butadiene, C_5H_8). Under non stress conditions only 1-2% of the carbon recently assimilated is emitted as isoprene, while, under stress conditions such as water scarcity, this value can reach up to 20-30% (*Q. pubescens*, Genard-Zielinski *et al.*, 2014). Although the role of isoprene is still under discussion, it seems likely that C_5H_8 helps plants to optimise CO_2 assimilation during temporary and mild stresses, especially during the growing and warmer periods (Loreto & Fineschi, 2015). The major role of isoprene in plant defence probably explains its large annual global emissions (440-660 $TgC.y^{-1}$, Guenther *et al.*, 2006), forming the largest quantity of all Biogenic Volatile Organic Compounds (BVOC) emitted. Although present in the atmosphere at the ppb or ppt level, isoprene has a broad impact on atmospheric chemistry, both in the gaz phase (especially in the O_3 budget of some urbanised areas) and in the particulate-phase (secondary organic aerosols formation) (Goldstein & Steiner, 2007), hence on the biosphere-atmosphere feedbacks.

It has extensively been shown that, under non-stressful conditions, isoprene synthesis and emission are tightly linked, and mainly dependent on the mere instantaneous light and temperature conditions (Guenther *et al.*, 1991, 1993). By contrast, isoprene emission and synthesis are uncoupled under stress environmental conditions which influence isoprene emissions in a way that is not completely understood and still under debate (Affek & Yakir, 2003; Peñuelas & Staudt, 2010). Whilst some authors highlighted an isoprene emission increase under mild water stress (Sharkey & Loreto, 1993; Funk *et al.*, 2004; Pegoraro *et al.*, 2004; Genard-Zielinski *et al.*, 2014), other studies report the opposite (Bruggemann & Schnitzler, 2002; Rodriguez-Calcerrada *et al.*, 2013; Tani *et al.*, 2011). Furthermore, isoprene emission intensity is also closely related to plant internal factors such as leaf ontogeny in deciduous species. The capacity of young leaves to release isoprene only occurs when a cumulated temperature threshold (degree day) is reached after bud breaking (Grinspoon *et al.*, 1991). Depending on the emitter and the location, this threshold was observed to range from 120 to 210 °C (*Salix phylicipholia*, Hakola *et al.*, 1998) to 400 °C (*Populus tremuloides*, Monson *et al.*, 1994). Moreover, after the emission onset, the seasonal variations of the leaf capacity to emit isoprene which can range over several orders of magnitude along the season

Biogeosciences Discuss., doi:10.5194/bg-2017-17, 2017
Manuscript under review for journal Biogeosciences
Discussion started: 9 February 2017

(Monson *et al.*, 1994, Geron *et al.*, 2000; Boissard *et al.*, 2001; Petron *et al.*, 2001; Hakola *et al.*, 1998).

Two main approaches have been considered so far to model isoprene emission variations: empirically-based parameterisations to represent the observed emission variations due to environmental drivers, and process-based relationships built on our understanding of the ongoing biological regulation (Ashworth *et al.*, 2013). Although both types of model are adapted for present day global/regional modelling, only the former ones are commonly used for atmospheric applications, especially for air quality exercises for which mechanistic models are far too complex. Although Grote *et al.* (2014) showed the ability of such models to account fairly well for mild stress effects on seasonal isoprene variations of *Quercus. ilex*., the high degree of descripting parameters required still represent an obstacle for their broad use in air quality and global scale emission exercises (Ashworth *et al.*, 2013). On the other hand, because the more widely used empirical models (see MEGAN: Model of Emissions of Gases and Aerosols from Nature, Guenther *et al.*, 2006) were developed using measurements made under 'optimum' growing conditions, it is still necessary to broaden their ability to assess isoprene emissions over a larger range of environmental conditions (including stress conditions) and variation frequencies (from high or instantaneous to low or seasonal). Such improvements imply ongoing updates as research studies go along and thereby require more advanced algorithms. In particular, MEGAN model is still struggling in considering the water availability (from precipitation or present in the soil) effects on isoprene emissions. Such a weakness can be particularly detrimental to isoprene emission inventories made over areas covered with a large quantity of high isoprene emitters and subject to frequent drought episodes, like the Mediterranean region. Besides, climate models predict over this area an amplification of the natural drought during summers due to a precipitation reduction which could, locally, reach up to 30% by the year 2100 (Giorgi & Lionello, 2008; IPCC 2013; Polade *et al.* 2014). Due to the strong interactions existing between air pollution over the large Mediterranean urban areas and strong BVOC emissions by local vegetation, the assessement of how global changes could impact isoprene emissions is a growing environmental issue to be adressed (Atkinson & Arey, 1998; Calfapietra *et al.*, 2009; Chameides *et al.*, 1988; Pacifico *et al.* 2009). In that context, a recent study underlines the importance of long-term monitorings of, both, isoprene emissions and soil moisture in water limited ecosystems (Zheng *et al.*, 2015). Since *Quercus pubescens* Willd. is the second isoprene emitter in Europe and the main one in the Mediterranean zone (Keenan *et al.* 2009),

Biogeosciences Discuss., doi:10.5194/bg-2017-17, 2017
Manuscript under review for journal Biogeosciences
Discussion started: 9 February 2017

it represents an ideal model species to further investigate the isoprene emission variability under drought conditions.

The objectives of this study were to (i) compare observed seasonal impacts of ND *vs* AD on *Q. pubescens* gaz exchanges (CO_2, H_2O) and isoprene emission rates (ER) at the O_3HP site, (ii) develop a specific isoprene emission algorithm taking into account drought (ND and AD) impacts on *Q. pubescens* ER, and, (iii) make some projections on the impacts of an AD of 30% on Downy oak ER over the Mediterranean area by the year 2100, under IPCC RCP2.6 (moderate) and RCP8.5 (extreme) scenarios.

2. Materials and methods

2.1 Experimental site O_3HP

Experimental data was obtained at the O_3HP site (Oak Observatory at the Observatoire de Haute Provence, 5°42'44" E, 43°55'54" N). This site is part of the French national network SOERE F-ORE-T (System of Observation and Experimentation, in the long term, for Environmental Research) dedicate to the forest ecosystem functioning. The O_3HP site (680 m above mean sea level) is located 60 km north of Marseille and consists of a homogeneous 70 year-old forest dominated by *Q. pubescens* (5 m height, LAI = 2.2) which accounts for ≈ 90% of the biomass and ≈75% of the trees. O_3HP facilities, in particular the rain exclusion system dynamically reducing precipitation by a deployable roof above the canopy, enabled to study this ecosystem under natural and amplified drought (averaging -30% of the annual cumulated precipitation), hereafter named 'ND' and 'AD' plot respectively. Ambient and soil environmental parameters were continuously monitored with a dense network of sensors (for details see section "COOPERATE environmental data base"). Access to the canopy was at two levels: ≈ 0.8 and 4 m (top canopy branches) above ground level, with the higher level being the focus of this study. Further description can be found in (Santonja *et al.* 2015).

2.2 Seasonal sampling strategy

Isoprene emission rate measurements were performed at least during one week, once a month, from June 2012 to June 2013, except from November 2012 to March 2013 when *Q. pubescent* is fully senescent with leaves remaining on the tree (marcescent species). This calendar allowed us to capture isoprene emissions during leaf maturity but also during bud break

Biogeosciences Discuss., doi:10.5194/bg-2017-17, 2017
Manuscript under review for journal Biogeosciences
Discussion started: 9 February 2017

(April 2013) and leaf senescence (October 2012). Three trees were studied in each plot along the whole seasonal cycle, with a single branch at the top of the canopy being mostly sampled for each tree. More intensive measurements were carried out in June 2012 (3 weeks) and April 2013 when tree-to-tree and within-canopy variability was assessed. One ND branch was sampled throughout all intensive campaigns, while the 5 other ND and AD branches were alternatively sampled during 1 to 2 days (Genard-Zielinski *et al.*, 2014). Isoprene samples were collected on cartridges packed with adsorbents, except in April 2013 where on-line isoprene measurements were performed using a PTR-MS directly connected to the enclosure via a 50 m length 1/4" PTFE line. When cartridges were used, samples were taken from sunrise to sunset, roughly every 2 hours. PTR-MS measurements allowed a higher sampling frequency (between 120 and 390 s^{-1}).

Branch enclosures were mostly installed on the previous day before the first emission rate measurement took place, and, at least, 2 h before.

2.3 COOPERATE environmental database

Ambient and edaphic parameters used for the artificial neural network (ANN) optimization were obtained from the COOPERATE database (https://cooperate.obs-hp.fr/db) and daily averaged for each day of our study. Ambient PAR (µmol m^{-2} s^{-1}) measured above the canopy at 6.5 m (Licor Li-190®; Lincoln, NE, USA) in the ND plot was used as the PAR reaching all the top canopy branches studied. Ambient air temperature (*T*, °C) measured at 6.15 m (multisensor Vaisalla) in the ND and AD plot was used for both sets of branches. Since some precipitation (*P*, mm) values were missing from the COOPORATE database during our data processing, P values from the nearby (< 10 km) Forcalquier meteorological station were used. Soil water content (SW, L L^{-1}) and temperature (ST, °C) at -0.1 m (Hydra Probe II SDI-12, Stevens, Water Monitoring Systems Inc., OR, USA) specific for each of the sampled trees were selected and extracted from the COOPORATE database. When data were missing, they were extrapolated from the nearest equivalent data point measurements. Daily mean PAR, *T*, *P*, SW and ST were cumulated over a time period ranging from 1 to 21 days before the measurement

2.4 Branch scale isoprene emissions and gas exchanges

Biogeosciences Discuss., doi:10.5194/bg-2017-17, 2017
Manuscript under review for journal Biogeosciences
Discussion started: 9 February 2017

Sampling was carried out using two identical dynamic branch enclosures (detailed description in Genard-Zielinski *et al.*, 2014). Briefly, the device consists of a ≈ 60 L PTFE (PolyTetraFluoroEthylene) frame closed by a sealed 50 µm thick PTFE film to which ambient air was introduced at Q_0 ranging between 11–14 L min^{-1} using a PTFE pump (KNF N840.1.2FT.18®, Germany). Gas flow rates were controlled by mass flow controllers (Bronkhorst) and all tubing lines were PTFE-made. A PTFE propeller ensured a rapid mixing of air inside the chamber. Microclimate (PAR, *T*, relative humidity) inside the chamber was continuously monitored (relative humidity and temperature probe LI-COR 1400–04®, and quantum sensor LI-COR, PAR-SA 190®, Lincoln, NE, USA) and recorded (Licor 1400®; Lincoln, NE, USA). CO_2/H_2O exchanges from the enclosed branches were also continuously measured using infrared gas analysers (IRGA 840A®, Licor) in order to assess the net assimilation P_n (in μmol_{CO2} m^{-2} s^{-1}) and the stomatal conductance to water vapour G_w (mol_{H2O} m^{-2} s^{-1}) using the equations from Von Caemmerer & Farquhar (1981) as detailed in Genard-Zielinski *et al.* (2015).

Total dry biomass matter (DM) was calculated by manually scanning every leaf of each sampled branch enclosed in the chamber and applying a dry leaf mass per area conversion factor (LMA) extrapolated from concomitant measurements made on the same site. Mean (range) DM was 0.16 (0.01 - 0.45) g_{DM}, and mean (range) AF was 13.17 (0.82 - 36.67) g_{DM} cm^{-2}.

Isoprene emission rates (ER) were calculated as:

$$ER = Q_0 \times (C_{out} - C_{in}) \times DM^{-1}, \quad (1)$$

where ER is expressed in µgC g_{DM}^{-1} h^{-1}, Q_0 is the flow rate of the air introduced into the chamber (L h^{-1}), C_{out} and C_{in} are the concentrations in the inflowing and outflowing air (µgC L^{-1}) and *DM* is the sampled dry biomass matter (g_{DM}).

All over the seasonal cycle, except in April, isoprene was collected using packed cartridges (glass and stainless-steel) prefilled with Tenax TA and/or Carbotrap. Isoprene was then analysed in the laboratory according to a gas chromatography–mass spectrometry procedure detailed in (Genard-Zielinski *et al.*, 2014), with a level of analytical precision better than 7.5%.

In April 2013, additionally to cartridges, two types of PTR-MS were used for on-line isoprene sampling and analysis. A quadrupole PTR-MS (HS-PTR-MS, Ionicon Analytik GmbH, Innsbruck Austria), connected to the ND branch enclosure, was operated at 2.2 mbar pressure, 60 °C temperature and a 500 V voltage in order to achieve an E/N ratio of ≈ 115 Td (E:

Biogeosciences Discuss., doi:10.5194/bg-2017-17, 2017
Manuscript under review for journal Biogeosciences
Discussion started: 9 February 2017

electric field strength (V cm^{-1}); N: buffer gas number density (molecule cm^{-3}); 1Td=10^{-17} V cm^2. The primary H_3O^+ ion count assessed at *m/z* 21 was 3 10^7 cps, with a typically < 10% contribution monitored from the first water cluster (*m/z* 37) and < 5% contribution from the O_2^+ (*m/z* 32). Measurements were operated in scan mode (*m/z* 21 to *m/z* 210) every 380 s. After 15 to 20 min of sampling of incoming air, the outgoing air was sampled for 30 to 60 min. A high resolution (m/Δm ≈ 4000) time of flight PTR-MS (PTR-ToF-MS-8000, Ionicon Analytik GmbH, Innsbruck Austria) connected to the second enclosure used in our study enabled to discriminate compounds when their masses differ at the tenth part. The main experimental characteristics were similar to the PTR-MS-Quad, but a 550 V voltage was used in order to reach an E/N ratio of ≈ 125 Td. The H_3O^+ ion count assessed at *m/z* 21 was 1.1 10^6 cps with a similar < 10% contribution monitored from the first water cluster (m/Z 37) and < 2.5% contribution from the O_2^+ (*m/z* 32). The signal at m/z 69 corresponding to protonated isoprene was converted into mixing ratio by using a proton transfer rate constant k of 1.96.10^{-9} $cm^3.s^{-1}$ (Cappellin *et al.*, 2012), the reaction time in the drift tube, and the experimentally determined ion transmission efficiency. The relative ion transmission efficiencies of both instruments were assessed using a standard gas calibration mixture (TO-14A Aromatic Mix, Restek Corporation, Bellefonte, USA; 100 ± 10ppb in nitrogen). Assuming an uncertainty of ±15 % in the k-rate constants and in the mass transmission efficiency, the overall uncertainty of the concentration measurement is estimated to be of the order of ±20 %. Background signal was obtained by passing air through a platinum catalytic converter heated at 300 °C. Detection limits defined as three times the standard deviation on the background signal were 10 and 50 ppt with the PTR-ToF-MS and the HS-PTR-MS respectively.

The overall uncertainty (sampling + analysis) on ER assessment was between 15 and 20%.

2.5 Statistics

All statistics were performed on STATGRAPHICS® centurion XV by Statpoint, Inc. Isoprene emission factors (I_s) under each plot were calculated as the slope of the linear regression between $C_L \times C_T$ (factors accounting for light and temperature variability of isoprene emissions respectively, as in Guenther *et al.*, 1993) and measured ER, with the exception of July when no such correlation was found (cf. Results). $C_L \times C_T$ were calculated using PAR and *T* recorded in the enclosure. Differences in P_n, G_w, ER and I_s between the ND and the AD plot were tested using U-Mann & Whitney tests). Seasonal changes in these

Biogeosciences Discuss., doi:10.5194/bg-2017-17, 2017
Manuscript under review for journal Biogeosciences
Discussion started: 9 February 2017

ecophysiological parameters were tested using Krusal-wallis test (K) and the analysis was performed separately on trees from the ND and AD plot. Comparisons between COOPORATE environmental data were made using a Wilcoxon test when data was not log-normal and a *t*-test when log-normal.

2.6 Artificial Neural Network (ANN)

The Artificial Neural Network (ANN) developed in this study was based on a commercial version of the Netral NeuroOne software v.6.0 (http://www.netral.com, France) used as a Multi-Layer Perceptron (MLP) in order to calculate multiple non-linear regressions between a set of input regressors x_i (the environmental variables measured at the O_3HP) and the output data y_{meas} (the measured isoprene ER). The assessed ER (y_{calc}) was calculated as follows:

$$y_{calc} = w_0 + \sum_{j=1}^{j=N}\left[w_{j,k} \times f\left(w_{0,j} + \sum_{i=1}^{i=n} w_{i,j} \times x_i\right)\right], \quad (2)$$

where w_0 is the connecting weight between the bias and the output, N the number of neurons N_j, f the transfer function, $w_{0,j}$ the connecting weight between the bias and the neuron N_j, w_i the connecting weight between the input and the neuron N_j, and x_i the n input regressors. The MLP optimisation of the weights w was achieved according to Boissard *et al.*, (2008). Every input regressor x_i was centrally-normalised. Two sub-datasets were considered, for the ND and AD plot respectively. For each sub-dataset, 80% of our data were used for training and optimising the MLP, and the overall 20% were used for blind validation based on root mean square error (RMSE). Training/validation splitting was made using a Kullback-Liebler distance function available in NeuroOne v 6.0. Only the nonlinear hyperbolic tangent (*tanh*) function was tested as transfer function f. Up to N=7 neurons were tested for every ANN setting. Overtraining phenomenon (a too large number of neurons *vs* the number of input parameters) was checked against the $RMSE_{training}/RMSE_{validation}$ evolution *vs* the number N of neurons tested.

2.7 Future climate data over the Mediterranean area and ORCHIDEE model description

For the present-day climate, T, P and PAR were assessed as the 2000-2010 daily averages and derived from the ISI–MIP (Inter-Sectoral Impact Model Intercomparison Project) climate data set (Warsz*aws*ki *et al.*, 2014) over the Mediterranean area which contains the bias-corrected

Biogeosciences Discuss., doi:10.5194/bg-2017-17, 2017
Manuscript under review for journal Biogeosciences
Discussion started: 9 February 2017

daily simulation output of the earth system model HadGEM2-ES. The corresponding data for the 2090-2100 period were derived from two ISI–MIP future projections forced along two Representative Concentration Pathways (RCPs): the so-called 'peak-and-decline' greenhouse gas concentration scenario RCP2.6 (optimistic scenario) and the 'rising' greenhouse gas concentration scenario RCP8.5 (extreme scenario). All *T*, *P* and PAR data were extracted for the entire Mediterranean region from the global ISI-MIP data set and subsequently averaged over the area.

SW and ST were assessed by running the global land-surface-model ORCHIDEE (ORganizing Carbon and Hydrology In Dynamic EcosystEms) over the European part of the Mediterranean region. Calculated SW and ST were averaged over this area. ORCHIDEE is a spatially explicit process-based model calculating the CO_2, H_2O, and heat fluxes exchanged between the land surface and the atmosphere. The processes in the model are represented at the time step of ½ hour basis, but the variations of water and carbon pools are calculated on a daily basis. Vegetation is described using 12 Plant Functional Types (PFT). Each PFT follows the same set of governing equations but takes different parameter values, except for the leafy season onset and offset, which are defined by PFT specific equations. A detailed description of the model is given in Krinner *et al.* (2005). Simulations over the European part of the Mediterranean region were performed with the ORCHIDEE model at 0.5 × 0.5° spatial resolution, using the soil parameters (clay, silt and sand fractions) from Zobler (1986) and since this study focuses on isoprene emissions from *Q. pubescens* we fixed the vegetation with the corresponding PFT 'temperate broad-leaf summer green tree'. The above-described ISI-MIP historical forcings and the ISI-MIP future projections were used as climate data. Equilibrium was reached by running ORCHIDEE on the first decade of the climate forcing (1961-1990) repeated in a loop, and the value of atmospheric CO_2 corresponding to the year 1961. Among the two different hydrology schemes available in ORCHIDEE the rather complex physically based 11-layer scheme was used (Guimberteau *et al.*, 2013).

3. Results

3.1 Environmental conditions observed at the O_3HP

Mean daily ambient air temperature *T* varied between -3 and 26 °C (January 2013 and August 2012 respectively, Fig. 1a). Seasonal PAR variations were in line with *T* variations, with daily means peaking at 900 µmol m^{-2} s^{-1} in July (Fig. 1b). In 2012, the amplification of the ND was

Biogeosciences Discuss., doi:10.5194/bg-2017-17, 2017
Manuscript under review for journal Biogeosciences
Discussion started: 9 February 2017

adjusted from May to reach its maximum (32%) in July and maintained until November when rain exclusion was stopped (Fig. 1c). The annual cumumaled *P* (P_{cum}) in the AD plot was lower by 273 mm than in the ND plot at the end of 2012 (782 compared to 509 mm). In 2013 the AD started only at the end of June, simulating a later amplification; our April and June 2013 measurements were thus not impacted by AD. From August to October 2012, SW was 50 to 90% lower in the AD plot than in the ND plot (≈ 0.02 and to 0.05 L_{H2O} L_{soil}^{-1} respectively in August, Fig. 1d). The AD plot soil water deficit remained significant until the end of the experiment (Mann & Whitney, $P<0.05$ in June 2012, $P<0.001$ from July 2012 to June 2013), although the rain exclusion system was not activated between December 2012 and June 2013.

No significant difference was noticed for monthly PAR and *T* means between the ND and the AD plot, except in September 2012 when branches sampled on the ND plot received significantly more PAR than branches on the AD plot (Mann & Whitney, $P<0.001$).

3.2 Physiology and isoprene seasonal variations

G_w and P_n showed similar seasonal patterns in both plots (Figs. 2a, 2b), with the lowest values in July-September (10-20 mol_{H2O} m^{-2} s^{-1} and ≈1 μmol_{CO2} m^{-2} s^{-1} respectively) and the highest in June (80-170 mol_{H2O} m^{2} s^{-1} and ≈9 μmol_{CO2} m^{-2} s^{-1} respectively). Respiration dominated over gross CO_2 assimilation in April, resulting in negative net assimilation (P_n ≈ -1 μmol_{CO2} m^{-2} s^{-1}) in both plots. By contrast, G_w and P_n were not similarly influenced by water stress. Whereas G_w was significantly reduced under AD since July 2012, P_n remained stable, expect in June 2013 when unexplained high P_n values twice higher under AD than ND were observed. This higher value was however attributed to only one of the AD branches and was, moreover, unlikely to be due to AD since rain exclusion started in 2013 after June.

Water stress impacted the ER seasonal pattern during summer alone (Fig. 2c). Maximum ER was one month delayed in the AD plot (104.8 µgC g_{DM}^{-1} h^{-1} in August) compared to the ND plot (78.5 µgC g_{DM}^{-1} h^{-1} in July). ER was the lowest in October (≈ 6 µgC g_{DM}^{-1} h^{-1} in both plots). During April bud-break and isoprene emission onset, ER was as low as 0.5 and 1 µgC g_{DM}^{-1} h^{-1} in the ND and AD plot respectively.

Although I_s was calculated every month as the slope of ER *vs* $C_L \times C_T$ (as in Guenther *et al.*, 1993), this correlation was not significant in July, especially for AD branches ($P>0.05$, R^2 = 0.06 and 0.01 for ND and AD respectively). As a result, I_s was assessed in July by averaging ER measured under environmental conditions close to 1000±100 µmol m^{-2} s^{-1} and 30±1 °C. In

Biogeosciences Discuss., doi:10.5194/bg-2017-17, 2017
Manuscript under review for journal Biogeosciences
Discussion started: 9 February 2017

general, AD branches showed poorer ER *vs* $C_L \times C_T$ correlations than branches growing in the ND plot (data not shown). I_s was significantly higher by a factor of 2 in August (P=3.9) and in September (P=3.9) for the AD branches compared to the ND (Fig. 2d). As for ER, I_s maximum was reached in August (137.8 µgC g_{DM}^{-1} h^{-1}) in the AD plot, while the maximum in the ND plot occurred in July (74.3 µgC g_{DM}^{-1} h^{-1}). The general high variability observed during the isoprene emission onset in April was as large as the AD-ND variability, and, thus, could not be attributed only to the water stress treatment. The annual I_s difference between ND and AD relatively to ND was +45%.

3.3 Modeling the isoprene seasonal variations

Because we were aiming at testing an isoprene emission model widely employed for air quality applications, the empirical MEGAN model (Model of Emissions of Gases and Aerosols from Nature, Guenther *et al.*, 2006) was tested to assess our observed seasonal and drought variability of ER. A value of 53 µgC g_{DM}^{-1} h^{-1} was used for the emission factor I_s as given by Simpson *et al.* (1999) for *Q. pubescens*, together with a wilting point θw of 0.138 m^3 m^{-3} (Chen & Dudhia, 2001). Some agreement between the calculated and the measured ER in the ND plot was found in June 2012 & 2013, October and April measurements (Fig. 3a), although June 2013 ER were strongly (more than a factor of 5) underestimated by MEGAN. In contrast, under AD, ER was correctly assessed by MEGAN only in June 2012. During the driest months (July, August, September), under ND and AD, SW recorded at the O_3HP (0.05 m^3 m^{-3}, see Fig. 1d) being lower than the θw used in MEGAN (0.138 m^3 m^{-3}) calculated ER were set to zero. When SW effect was not selected in MEGAN, an overall understimation of 60 and 70% was still found in the ND and AD plots respectively, and no more than 50% of the seasonal variations were captured (data not shown).

Among the different ANN settings tested, the *G*14 optimised architecture (lowest RMSE, no overtraining, best correlation between measured and calculated ER over the whole range of value, see Boissard *et al.*, 2008) was found for N=3 and a set of 16 x_i with their corresponding connecting weights w_i (Appendices 1). More than 80% of the ER seasonal variations were assessed by *G*14, whatever the water stress (ND or AD) and the month, except in July (Fig. 3b) when ER were always poorly represented whatever the different ANN settings considered.

Biogeosciences Discuss., doi:10.5194/bg-2017-17, 2017
Manuscript under review for journal Biogeosciences
Discussion started: 9 February 2017

Among the environmental regressors used in *G*14, SW was found – whatever the frequency considered - to be the dominant parameter to explain the observed ER seasonal variations, especially when *Q. pubescens* was growing under AD (Fig. 4a). When water stress became significant in July, ER seasonal variations were found to be more sensitive to higher frequency changes in the environmental conditions (0 to 7 days before the measurement), whatever the regressors used, compared to April and June when ER were more sensitive to lower frequencies (14 to 21 days) for both ND and AD (Fig. 4b). On the overall, *T* and *L*, whatever their frequencies but in particular when considered instantaneously, did not account for more than 15% in the seasonal ER pattern.

3.4 2100 projections over the European Mediterranean

Relative changes between present and future climates were averaged on a monthly basis for the climate parameters used in *G*14 (SW, ST, *T*, PAR and *P*) and ER, according to the RCP2.6 and RCP8.5 scenarios (Fig. 5). PAR changes between present and future climates being negligible for both scenarios they are therefore not presented. Among the different *G*14 parameters, the highest monthly relative changes was found for *P* (+80% in March, RCP2.6) and ST (+105 and +120% in January and December respectively; RCP8.5, Fig. 5a).

The annual P_{cum} was found to be 1401 and 758 mm according to the RCP2.6 and RCP 8.5 projections respectively (data not shown), leading to an annual P_{cum} relative change of +6% and -24% for RCP2.6 and RCP8.5 respectively (Fig. 5a). Major *P* relative changes occur in late winter for RCP2.6 (a 50% increase) and during the summer for RCP8.5 (a strong decrease down to -90% in August). SW relative change profiles were found to be in line with *P*.

T relative changes were found to be always positive according to both scenarios, with an annual relative increase of 11% (+1.5 °C) and 41% (+5.4 °C) for the RCP2.6 and RCP 8.5 respectively (Fig. 5a). For both scenarios the strongest monthly changes were observed during the winter time (+50% and +87% in December for RCP2.6 and RCP 8.5 respectively), while the summer $\Delta T/T$ was of the order of +10 and +40% respectively. The ST relative change profiles were found to be in line with *T*.

Monthly changes of ER calculated using *G*14 ($d\mathrm{ER}_{G14}$) generally increased under both scenarios, but more intensively under the extreme RCP8.5 (up to +52.8 and +13.8 µgC g_{DM}^{-1} h^{-1} in August for RCP2.6 and RCP8.5 respectively, Fig. 5b). The highest $d\mathrm{ER}_{G1}$ decreased was assessed in September for RCP2.6 (-2.4 µgC g_{DM}^{-1} h^{-1}, Fig. 5b). The corresponding

Biogeosciences Discuss., doi:10.5194/bg-2017-17, 2017
Manuscript under review for journal Biogeosciences
Discussion started: 9 February 2017

monthly relative changes ($d\mathrm{ER}_{G14}/\mathrm{ER}_{G14}$) were maximal in July (+500%) and October (+800%) according to RCP2.6 and RCP8.5 respectively (Fig. 5c). On the overall, $d\mathrm{ER}_{G14}/\mathrm{ER}_{G14}$ was +70 and +320% for RCP2.6 and RCP8.5 respectively.

Whatever the projections, $d\mathrm{ER}_{G14}/\mathrm{ER}_{G14}$ was found to be relatively more impacted by water availability *W* (calculated as the sum of relative impact of SW and *P*) than by temperature effect (calculated as the sum of relative impact of ST and *T*): 67 and 63% for RCP2.6 and RCP8.5 respectively (Fig. 5d). By contract, temperature contribution became higher (more than 60%) in October and June under RCP2.6 and RCP8.5 respectively.

Whatever the *G*14 parameters used, the seasonal variations of $d\mathrm{ER}_{G14}/\mathrm{ER}_{G14}$ were mainly affected by 14-d frequencies (36.8 %, Fig. 5e), especially during early spring (65%) under the RCP2.6 scenario, while instantaneous variations of the *G*14 parameters became predominant (30.3 %) for the RCP8.5, and especially during summer (50 %). The lowest frequency (21-d) impact was similar for both scenarios and was close to 10% over the season

4. Discussion

4.1 Water stress impacts on the seasonal gas exchange of Q. pubescens

Despite a significant G_w reduction in summer 2012 due to the AD, *Q. pubescens* maintained a positive P_n during all summer, regardless of the water stress (ND or AD). Such behaviour enables trees to limit the evapotranspiration under water stress and, as a drought-acclimated species, to ensure enough carbohydrates accumulation for winter (Chaves *et al.*, 2002). Such strategy was also observed in a study conducted on the same species but under greenhouse conditions (Genard-Zielinski *et al.*, 2014). The seasonal regulation/conservation of P_n and G_w enabled isoprene emissions to be maintained even during the summer water stress (ND and AD). The observed significant increase (a factor of 2) of the tree capacity to emit isoprene under AD (August and September) illustrates how isoprene is likely to be important for short-term *Q. pubescens* drought-resistance, in particular through the ability of isoprene to stabilise the thylakoids membrane, under, for example, a thermal or oxidative stress as shown for *Populous* species (Velikova *et al.*, 2012). Previous studies highlighted the possibility for a plant growing under a water stress to synthesise isoprene using an alternative carbon source (extra-chloroplastic carbohydrates, Lichtenthaler *et al.*, 1997; Funk *et al.*, 2004). Interestingly, the maximum I_s value was very similar for both treatments (≈ 140 $\mu g.g_{DM}^{-1}.h^{-1}$) but was reached one month later under the AD (August compared to July). These observations

Biogeosciences Discuss., doi:10.5194/bg-2017-17, 2017
Manuscript under review for journal Biogeosciences
Discussion started: 9 February 2017

strengthen the hypothesis that, under environmental stresses (like water stress), some plants favour the allocation of carbon to secondary metabolites production (such as isoprene) rather than allocation to growth. Maximum I_s was very close to previously measured values obtained for the same species under Mediterranean conditions during greenhouse and *in-situ* experiment (114.3 and 134.7 $\mu g.g_{DM}^{-1}.h^{-1}$, Genard-Zielinski *et al.*, 2014; Simon *et al.*, 2005 respectively). The difference observed in April 2013 between I_s in the ND and AD plot cannot be attributed only to the AD effect, since the rain exclusion was started only at the end of June 2013; apart from a possible 'memory effect', it is likely due to the high natural variability in bud breaking and isoprene emission onset at this period of the year.

The strong uncoupling between ER and $C_L \times C_T$ reported for July measurements occurred when soil water content conditions significantly decreased at the O_3HP, in both plots, down to their seasonal minimum values (0.05 and 0.03 $m^3\ m^{-3}$). Such an uncoupling was also observed for some other strong isoprene emitters under water stress (*Quercus serrata* Murray and Blume, *Quercus crispula*, Tani *et al.*, 2011). It confirms the assumption of these authors that extra-chloroplastic isoprene precursors supply the carbon basis for isoprene biosynthesis (and not only from CO_2 fixed instantaneous in the chloroplast) when water stress occurs, explaining why isoprene emissions become less dependent of the classical abiotic factors PAR and T considered in the empirical MEGAN model, or the other environmental abiotic regressors tested in this study. However, our statistical approach used in this study would require a larger set of data to further investigate this particular point.

4.2 Towards what isoprene emission modeling improvement?

Since most of the empirical isoprene emission algorithms of MEGAN have been developed from measurements carried out under 'optimal' (*i.e.* 'none stressing') conditions, they still show difficulties in capturing the impacts of various stress conditions, such as the water deficit, for instance. Hence, ER measured during this study, was observed to be rarely dependent on T and PAR only: indeed, except in June (e.g. just before the ND and AD onset), MEGAN was unable to predict isoprene emission variations. In particular in July, the strong uncoupling between ER and $C_L \times C_T$ illustrates the extent to which other additional parameters than the abiotic parameters T and PAR should be taken into account in isoprene MEGAN algorithm in order to better capture the shift from carbon allocation to growth towards secondary metabolites synthesis during reduced water availability conditions.

Biogeosciences Discuss., doi:10.5194/bg-2017-17, 2017
Manuscript under review for journal Biogeosciences
Discussion started: 9 February 2017

Our approach in developing a specific algorithm for *Q. pubescens* (*G*14) confirmed the strong impact of the soil water content in the Mediterranean area, and not only under stress conditions. However, the SW effect as considered in the MEGAN isoprene model was found to be not adapted to account for *Q. pubescens* capacity to resist to water stress: isoprene emissions did not decrease nor cease under ND or AD conditions as expected in summer by MEGAN; on the contrary, they were observed to be maintained, and even increased, during the maximum AD period when SW became lower than the wilting point θw. Since the SW availability modulation (1 to 0) used in MEGAN was based on the single observation made by Pegoraro *et al.* (2004) between *Populus deltoids* photosynthesis and stomatal conductance to water vapour, it is obviously not appropriate for water stress-resistant species. Such a discrepancy under conditions other than Mediterranean was also noticed by Potosnak *et al.*, 2014) during a seasonal study over a mixed broad-leaf forest mainly composed of *Q. alba* L. and *Q. velutina* Lam. (Missouri, USA). Although they found that MEGAN robustly captured 90% of the observed variance during most of the annual cycle, it was unable to reproduce the time-dependent response of isoprene emission to water stress (θw of 0.084 m^3 m^{-3}). Improved isoprene empirical models should be able to more realistically account for the drought adaptation by the emitter. One way could be, for MEGAN, to add an emitter-dependent parameter in the general isoprene algorithm. Moreover, Guenther *et al.* (2013) suggested that including soil moisture averaged over longer time periods (such as the previous month and not only the mean over the previous 240h) may help to yield better predictions during drought periods. Note that MEGAN performed better on our experimental data when its SW modulation was set to 1 (no SW effect), since almost half of the isoprene variations were then assessed, whatever the water stress intensity; however a general underestimation of a factor of 2 remained (data not shown).

Our work also highlighted the seasonal change occurring in the regulation frequency of isoprene emissions, especially when stressed environmental conditions appeared. Indeed, *Q. pubescens* isoprene emissions became more highly sensitive to rapid environmental changes as drought intensity increased: in June 2012, ER_{G14} variations were mainly controlled by a 14-day frequency (under ND and AD) while they became later in the season mainly 7-day, and even 0- to 7-day dependent as soon as the ND and AD, respectively, increased (Fig. 4). Moreover, only a small fraction of ER_{G14} variations were due to instantaneous environmental variations changes (as mostly accounted for in MEGAN). The highlighting of a dynamical regulation over oak seasonal leaf development and of a lower than instantaneous frequency dependency of their isoprene emission was also made for *Q. alba* and *Q.*

macrocarpa (Geron *et al.*, 2000; Petron *et al.*, 2001 respectively): isoprene onset was observed to also strongly correlate with ambient temperature cumulated over ≈2 weeks (200 to 300 degree day, d.d., °C) while maximum ER was observed at 600-700 d.d. °C. If part of this dynamical regulation is already included in the leaf age emission activity $\gamma_{A,i}$ of MEGAN isoprene emission algorithm, the part due to the impacts of stressing conditions is not yet considered, and not only when the plant is experiencing a drought period. For instance, Wiberley *et al.* (2005) observed that the onset of kudzu isoprene emissions were shortened by one week under elevated temperature compared to cold growth.

On one side, and as suggested by Zheng *et al.* (2015), ad-hoc long-term direct measurements of isoprene emission as the one performed at the O_3HP, are still essential to provide further information for empirical model improvement on how isoprene emissions are seasonally affected by water availability. However, on the other side, representation of soil moisture in land-surface and climate models is currently poor (Köstner *et al.*, 2008). Consequently, further actions need to be undertaken in order to provide a better description of soil moisture at the surface (*e.g.* the NASA Soil Moisture Active Passive instrument) and thus improve the representation of the effective water available for plants in emission models.

4.3 What future impacts of amplified drought on isoprene emissions?

Depending on the future scenario tested, changes in precipitation (thus in soil water content) and/or in temperature will differently affect the Mediterranean area tested in our study.

A net P_{cum} reduction was predicted only under the extreme CO_2 trajectories RCP8.5, with an annual decrease of 24%, similar to the AD applied at the O_3HP site during our study (-30% of precipitation), together with strong temperature increase (+5.4 °C). On the contrary, the only main change predicted under the RCP2.6 scenario was a moderate temperature increase (+1.5 °C), whereas the annual predicted P_{cum} remained more or less stable (a slight +6% increase, due to heavier rain falls in winter). In terms of AD, the O_3HP experimental strategy followed during this work illustrated the upper limit of the drought intensity that *Q. pubescens* should undergo on the 2100 horizon in the Mediterranean area.

The mere RCP2.6 *T* increase had a similar predicted impact on ER_{G14} relative change (+70%) than the mere precipitation reduction had on our observed ER (+45%). If an isoprene emission increase is generally predicted and observed in relation with future temperature enhancement (Peñuelas & Staudt, 2010), such a response seems not so clear under Mediterranean water deficit conditions (Llusià *et al.*, 2008, 2009). In our case, when the

Biogeosciences Discuss., doi:10.5194/bg-2017-17, 2017
Manuscript under review for journal Biogeosciences
Discussion started: 9 February 2017

combined effects of temperature and drought increase were considered (RCP8.5 scenario), the predicted ER_{G14} relative changes were enhanced compared to the sum of the individual relative effects of drought and temperature: on the average, ER_{G14} was multiplied by a factor of 3 (RCP8.5, Fig. 5c). During summer, this enhancement was particularly pronounced when the drought became maximum (August) with ER_{G14} relative changes nearly 10 times higher under the RCP8.5 than the RCP2.6 (+430 and +46% respectively). Yet, the highest predicted enhancement occurred when the drought period ended, in October, with ER_{G14} increased by a factor of 8 under RCP8.5. In addition to expected high dER_{G14}/ER_{G14} values during the drought period, the main relative change in isoprene emission would actually occur in autumn. This prediction is in agreement with observations made on different emitters in the Mediterranean area where isoprene emissions were observed in autumn to reach levels as high as in spring as soon as the water stress is declining and the net assimilation, hence the isoprene emissions, are favored again (*e.g*. Owen *et al.*, 1998). Moreover, the relative effect of *T* on dER_{G14} was predicted to increase and became even higher (up to 64%, RCP2.6) or similar (RCP8.5, Fig. 5d) to the *W* relative effect in October, as soon as drought intensity lowered: ER and *T* variations became, again, highly coupled as in the current isoprene algorithms (*e.g*. G95, Guenther *et al.*, 1995). However, in June, the relative higher *T* effect on dER_{G14} compared to *W* (60 *vs* 40%, RCP8.5, Fig. 5d) could illustrate a higher sensitivity of *Q. pubescens* isoprene emissions to temperature stress as the drought is setting in. Such a co-effect was also observed by Genard-Zielinski (2014) on *Q. pubescens* branches that were growing in the AD plot. Except in June and October, dER_{G14}/ER_{G14} seasonal variations were predicted to become mainly driven by the water budget (more than 65%) compared to temperature (less than 35%), whatever the scenario used.

These 2100 projections were made considering an unchanged *Q. pubescens* biomass, *i.e.* not affected by long term acclimation to *T* and drought increase. However, one can question, on the one hand, if *Q. pubescens* could maintain such a high allocation of its primary assimilated carbon (primary plant metabolites, PPMs) to isoprene emissions (secondary plant metabolites, PSMs). Indeed, for a constant assimilation, the PSMs/PPMs ratio could, on the overall, be multiplied by up to a factor of 3, and could reach a 7 fold increase during the highest drought periods (Saunier *et al.*, under review). Genard-Zielinski *et al.* (2014) showed that, under moderate and severe drought, *Q. pubescens* aerial and foliar growth was negatively affected. Furthermore, on a long term, such a cost could impact the overall energy budget and speed up the plant senescence (Loreto & Schnitzler, 2010). Our predicted isoprene emission increases could then be offset, or even reversed. On the other hand, one should also consider the

additional co-effects of the CO_2 increase expected a year by 2100. Bytnerowicz *et al.* (2007) reported that, if the temperature increase would have little effect, an elevated CO_2 would favor both growth and water use efficiency of plants, and account for a 15-20% increase on forest NPP. When CO_2 enhancement was considered, the leaf mass (g) per square meter of the PFT ground (broad leaf temperate) tested in ORCHIDEE during this work was predicted to, relatively, increase by 35 and 100 % under RCP2.6 and RCP8.5 respectively. Tognetti *et al.* (1998) observed a similar positive effect on the assimilation rate of both *Q. pubescens* and *Q. ilex* during a long term CO_2 enhancement study, and measured a net increase in the diurnal course of isoprene emissions.

Understandably, the *G*14 algorithm should be validated on a longer period of measurements in order to assess how *Q. pubescens* acclimate over a longer period of drought, and confirm or deny these projections. In that context, since June 2013, measurements have been continued at the O_3HP on the same branches as the ones studied in this study (Saunier *et al.*, under review). However, the major impact of the future climate changes (higher drought, temperature and CO_2) on isoprene emissions could, eventually, be related to the expected general land cover change, with a shift of the actual Mediterranean species to more favorable conditions. Such impacts can only be assessed with - improved - isoprene emission models coupled with global dynamic vegetation models.

Acknowledgements. We are particularly grateful to P. E. Blanc, J. C. Brunel G. Castagnoli, A. Rotereau and other OHP staff for support before and during the different campaigns. We thank members of the DFME team from IMBE: S. Greff, C. Lecareux, S. Dupouyet and A. Bousquet-Melou for their help during measurements and analysis. This work was supported by the French National Agency for Research (ANR) through project CANOPÉE (ANR-2010 JCJC 603 01) and project SecPriMe^2 (ANR-12-BSV7-0016-01), INSU (ChARMEx), CNRS National program EC2CO-BIOEFECT (ICRAM project), CEA, and Université Paris Diderot-Paris 7. We are grateful to ADEME/PACA for PhD funding. For O_3HP facilities, the authors thank the research federation ECCOREV FR3098 and the LABEX OT-Med (no. ANR-11-LABEX-0061) funded by the French Government through the A*MIDEX project (no. ANR-11-IDEX-0001-02). The authors thank the MASSALYA instrumental platform (Aix Marseille Université, lce.univ-amu.fr) for the analysis and measurements used in this publication

Biogeosciences Discuss., doi:10.5194/bg-2017-17, 2017
Manuscript under review for journal Biogeosciences
Discussion started: 9 February 2017

References

Affek, H. P. and Yakir, D.: Natural abundance carbon isotope composition of isoprene reflects incomplete coupling between isoprene synthesis and photosynthetic carbon flow, Plant Physiol., 131, 1727–1736, 2003.

Ashworth, K., Boissard, C., Folberth, G., Lathière, J., and Schurgers, G.: Global modelling of volatile organic compound emissions, in: Biology, Controls and Models of Tree Volatile Organic Compound Emissions, Tree Physiology 5, edited by Niinemets, Ü., Monson, R.K., Springer Science + Business Media, Dortrecht, The Netherlands, 451–487, 2013

Atkinson, R. and Arey, J.: Atmospheric chemistry of biogenic organic compounds. Accounts Chem. Res., 31, 574–583, 1998.

Blanch, J. S., Peñuelas, J., Sardans, J., and Llusià, J.: Drought, warming and soil fertilization effects on leaf volatile terpene concentrations in Pinus halepensis and Quercus ilex, Acta Physiol. Plant, 31, 207–218, 2009.

Boissard, C., Cao, X. L., Juan C. Y., Hewitt, C. N., and Gallagher, M.: Seasonal variations in VOC emission rates from gorse (Ulex europaeus), Atmos. Environ., 35, 917–927, 2001.

Boissard, C., Chervier, F., and Dutot, A. L.: Assessment of high (diurnal) to low (seasonal) frequency variations of isoprene emission rates using a neural network approach, ACP., 8, 2089–2101, 2008.

Brüggemann, N. and Schnitzler, J.: Comparison of isoprene emission, intercellular isoprene concentration and photosynthetic performance in water-limited oak (Quercus pubescens Willd. and Quercus robur L.) saplings, Plant Biol., 4, 456–463, 2002.

Bytnerowicz, A., Omasa, K., and Paoletti, E.: Integrated effects of air pollution and climate change on forests: A northern hemisphere perspective, Environ. Pollut., 147, 438–445, 2007.

Calfapietra, C., Fares, S., and Loreto, F.: Volatile organic compounds from Italian vegetation and their interaction with ozone, Environ. Pollut., 157, 1478–1486, 2009.

Cappellin, L., Karl, T., Probst, M., Ismailova, O., Winkler, P. M., Soukouli, C., Aprea, E., Maerk, T. D., Gasperi, F., and Biasioli F.: On quantitative determination of volatile organic compound concentrations using Proton Transfer Reaction Time-of-Flight Mass Spectrometry, Environ. Sci. Technol., 46, 2283–2290, 2012.

Chameides, W. L., Lindsay, R. W., Richardson, J., and Kiang, C. S.: The role of biogenic hydrocarbons in urban photochemical smog - Atlanta as a case-study, Science, 241, 1473–1475, 1988.

Chaves, M. M., Pereira, J. S., Maroco, J., Rodrigues, M. L., Ricardo, C. P. P., Osorio, M. L., Carvalho, I., Faria, T., and Pinheiro, C.: How plants cope with water stress in the field. Photosynthesis and growth, Ann. Bot., 89, 907–916, 2002.

Chen, F., and Dudhia, J.: Coupling an advanced land surface-hydrology model with the Penn State-NCAR MM5 modeling system, Part I: Model implementation and sensitivity, Mon. Weather Rev., 129, 569–585, 2001.

Funk, J. L., Mak, J. E., and Lerdau, M. T.: Stress-induced changes in carbon sources for isoprene production in Populus deltoides, Plant Cell Environ., 27, 747–755, 2004.

Genard-Zielinski, A. C., Ormeño, E., Boissard, C., and Fernandez, C.: Isoprene emissions from Downy Oak under water limitation during an entire growing season: what cost for growth? PLoS ONE, 9 (11): e112418. doi:10.1371/journal.pone.0112418, 2014.

Genard-Zielinski, A. C., Fernandez, C., Boissard, C., Kalokridis, C., Gros, V., Lathière, J., Orts, JP., Greff, S., Bonnaire, N., and Ormenõ, E.: Variability of BVOC emissions from a Mediterranean mixed forest in southern France with a focus on Quercus pubescens, ACP., 14, 17225–17261, 2015.

Geron, C., Guenther, A. B., Sharkey, T., and Arnts, R. R.: Temporal variability in basal isoprene emission factor, Tree Physiol., 20, 799–805, 2000.

Giorgi, F. and Lionello, P.: Climate change projections for the Mediterranean region, Global Planet. Change, 63, 90–104, 2008.

Goldstein, A. and Steiner, A. H.: Biogenic VOCs, in: Volatile Organic Compounds in the Atmosphere, Koppmann R., (Ed), Blackwell Publishing Ltd, Oxford, UK, 82-128, 2007.

Grinspoon, J., Bowman, W. D., and Fall, R.: Delayed onset of isoprene emission in developing velvet bean (Mucuna sp.) leaves, Plant Physiol., 97, 170–174, 1991.

Grote, R., Morfopoulos, C., Niinemets, U., Sun, Z., Keenan, T. F., Pacifico, F., and Butler, T.: A fully integrated isoprenoid emissions model coupling emissions to photosynthetic characteristics, Plant Cell Environ., 37, 1965–1980, 2014.

Guenther, A. B., Hewitt, C. N., and Erickson, D., Fall, R., Geron, C., Graedel, T., Harley, P., Klinger, L., Lerdau, M., Mckay, W. A., Pierce, T., Scholes, B., Steinbrecher, R., Tallamraju, R., Taylor, J., and Zimmerman, P.: A global-model of natural volatile organic-compound emissions, J. Geophys. Res-Atmos., 100, 8873–8892, 1995.

Guenther, A. B., Karl, T., Harley, P., Wiedinmyer, C., Palmer., PI, and Geron, C. Estimates of global terrestrial isoprene emissions using MEGAN (Model of Emissions of Gases and Aerosols from Nature), ACP., 6, 3181–3210, 2006a.

Guenther, A. B., Monson, R. K., and Fall, R.: Isoprene and monoterpene emission rate variability - Observations with Eucalyptus and emission rate algorithm development, J. Geophys. Res-Atmos., 96, 10799–10808, 1991.

Guenther, A. B., Zimmerman, P. R., Harley, P. C., Monson, R. K., and Fall, R.: Isoprene and Monoterpene Emission Rate Variability - Model Evaluations and Sensitivity Analyses, J. Geophys. Res-Atmos., 98, 12609–12617, 1993.

Guimberteau, M., Ronchail, J., Espinoza, J. C., Lengaigne, M., Sultan, B., Polcher, J., Drapeau, G., Guyot, J. L., Ducharne, A., and Ciais, P.: Future changes in precipitation and impacts on extreme streamflow over Amazonian sub-basins, Environ. Res. Lett., 8(1), 014040, 2013.

Hakola, H., Rinne, J., and Laurila, T.: The hydrocarbon emission rates of tea-leafed willow (Salix phylicifolia), silver birch (Betula pendula) and European aspen (Populus tremula), Atmos. Environ., 32, 1825–1833, 1998.

IPCC Climate Change 2013: The Physical Science Basis. Contribution of Working Group I to the Fifth Assessment Report of the Intergovernmental Panel on Climate Change, Stocker, T. F., Qin, D., Plattner, G. K., Tignor, M., Allen, S. K., Boschung, J., Nauels, A., Xia, Y., Bex, V., and Midgley, P. M., (Eds), Cambridge University Press, Cambridge, United Kingdom and New York, NY, USA, 1535pp., 2013.

Keenan, T., Niinemets, U., Sabate, S., Gracia, C., and Peñuelas, J.: Process based inventory of isoprenoid emissions from European forests: model comparisons, current knowledge and uncertainties, ACP., 9, 4053–4076, 2009.

Köstner, B., Matyssek, R., Heilmeier, H., Clausnitzer, F., Nunn, A. J., and Wieser, G.: Sap flow measurements as a basis for assessing trace-gas exchange of trees, Flora, 203, 14–33, 2008.

Krinner, G., Viovy, N., de Noblet-Ducoudre, N., Ogee, J., Polcher, J., Friedlingstein, P., Ciais, P., Sitch, S., and Prentice, I.: A dynamic global vegetation model for studies of the coupled atmosphere-biosphere system, Global Biogeochem. Cy., 19, GB1015, 2005.

Lichtenthaler, H. K., Schwender, J., Disch, A., and Rohmer, M.: Biosynthesis of isoprenoids in higher plant chloroplasts proceeds via a mevalonate-independent pathway, FEBS Lett., 400, 271–274, 1997.

Llusià, J., Peñuelas, J., Alessio, G., and Estiarte, M.: Contrasting species‐specific, compound‐specific, seasonal and interannual responses of foliar isoprenoid emissions to experimental drought in a Mediterranean shrubland, Int. J. Plant Sci., 169, 637–645, 2008.

Loreto, F. and Fineschi, S.: Reconciling functions and evolution of isoprene emission in higher plants, New Phytol., 206, 578–582, 2015.

Loreto, F. and Schnitzler, J-P.: Abiotic stresses and induced BVOCs, Trends Plant Sci., 15, 154–166, 2010.

Monson, R. K., Harley, P. C., Litvak, M. E., Wildermuth, M., Guenther, A. B., Zimmerman, P. R., and Fall, R.: Environmental and developmental controls over the seasonal pattern of isoprene emission from aspen leaves, Oecologia, 99, 260–270, 1994.

Owen, S., Boissard, C., Hagenlocher, B., and Hewitt, C.: Field studies of isoprene emissions from vegetation in the Northwest Mediterranean region, J. Geophys. Res., 103, 25499–25511, 1998.

Pacifico, F., Harrison, S. P., Jones, C. D., and Sitch, S.: Isoprene emissions and climate, Atmos. Environ., 43, 6121–6135, 2009.

Pegoraro, E., Rey, A., Greenberg, J., Harley, P. C., Grace, J., Malh, Y., and Guenther, A. B.: Effect of drought on isoprene emission rates from leaves of Quercus virginiana Mill, Atmos. Environ., 38, 6149–6156, 2004.

Peñuelas, J. and Staudt, M.: BVOCs and global change, Trends Plant Sci., 15, 133–144, 2010.

Petron, G., Harley, P. C., Greenberg, J., and Guenther, A. B.: Seasonal temperature variations influence isoprene emission, Geophys. Res. Lett., 28, 1707–1710. 2001.

Polade, S. D., Pierce, D. W., Cayan, D. R., Gershunov, A., and Dettinger, M. D.: The key role of dry days in changing regional climate and precipitation regimes, Sci. Rep., 4, 4364, 2014.

Potosnak, M. J., LeStourgeon, L., Pallardy, S. G., Hosman, KP., Gu, L., Karl, T., Geron, C., and Guenther, A. B.: Observed and modeled ecosystem isoprene fluxes from an oak-dominated temperate forest and the influence of drought stress, Atmos. Environ., 84, 314–322, 2014.

Rodriguez-Calcerrada, J., Buatois, B., Chiche, E., Shahin, O., and Staudt, M.: Leaf isoprene emission declines in Quercus pubescens seedlings experiencing drought - Any implication of soluble sugars and mitochondrial respiration? Environ. Exp. Bot., 85, 36–42, 2013.

Santonja, M., Fernandez, C., Gauquelin, T., and Baldy, V.: Climate change effects on litter decomposition: intensive drought leads to a strong decrease of litter mixture interactions, Plant Soil, 393, 69-82, 2015.

Saunier, A., Ormeño, E., Boissard, C., Wortham, H., Temime-Roussel, B., Lecareux, C., Armengaud, A., and Fernandez, C.: Effect of mid-term drought on BVOCs emission seasonality in Quercus pubescens and their dependence to light and temperature, ACP, in review.

Sharkey, T. D., and Loreto, F.: Water-stress, temperature, and light effects on the capacity for isoprene emission and photosynthesis of kudzu leaves, Oecologia, 95, 328–333, 1993.

Simon, V., Dumergues, L., Solignac, G., and Torres, L.: Biogenic emissions from Pinus halepensis: a typical species of the Mediterranean area, Atmos. Environ., 74, 37–48, 2005.

Simpson, D., Winiwarter, W., Börjesson, G., Cinderby, S., Ferreiro, A., Guenther, A., Hewitt, C.N., Janson, R., Khalil, M.A.K., Owen, S., Pierce, T.E., Puxbaum, H., Shearer, M., Skiba, U., Steinbrecher, R., Tarrasón, L., and Öquist, M.G.: Inventorying emissions from nature in Europe, J. Geophys. Res-Atmos., 104, 8113–8152. doi:10.1029/98jd02747, 1999.

Tani, A., Tozaki, D., Okumura, M., Nozoe, S., and Hirano, T.: Effect of drought stress on isoprene emission from two major Quercus species native to East Asia. Atmos. Environ., 45, 6261–6266, 2011.

Tognetti, R., Longobucco, A., Miglietta, F., and Raschi, A.: Transpiration and stomatal behaviour of Quercus ilex plants during the summer in a Mediterranean carbon dioxide spring, Plant Cell Environ., 21, 613-622, 1998.

Velikova, V., Sharkey, T. D., and Loreto, F.: Stabilization of thylakoid membranes in isoprene-emitting plants reduces formation of reactive oxygen species, Plant Signal. Behav., 7, 139–141, 2012.

Voncaemmerer, S. and Farquhar, G. D.: Some relationships between the biochemistry of photosynthesis and the gas-exchange of leaves, Planta, 153, 376–387, 1981.

Warszawski, L., Frieler, K., Huber, V., Piontek, F., Serdeczny, O., and Schewe, J.: The Inter-Sectoral Impact Model Intercomparison Project (ISI-MIP): Project framework, PNAS., 111, 3228–3232, 2014.

Wiberley, A., Linskey, A., Falbel, T., and Sharkey, T.: Development of the capacity for isoprene emission in kudzu, Plant, Cell Environ., 28, 898–905, 2005.

Zheng, Y., Unger, N., Barkley, M. P., and Yue, X.: Relationships between photosynthesis and formaldehyde as a probe of isoprene emission, ACP., 15, 8559–8576, 2015.

Zobler, L.: A world soil file for global climate modelling, NASA Technical Memorandum, NASA 87802, New York, U.S.A, 1986.

Biogeosciences Discuss., doi:10.5194/bg-2017-17, 2017
Manuscript under review for journal Biogeosciences
Discussion started: 9 February 2017

Figure caption

Figure 1.: Seasonal variations of daily environmental parameters measured at the O_3HP from March 2012 to July 2013. (a) Ambient air temperature *T* was obtained at 6.5 m above ground level (a.g.l.), approximatively 1.5 m above the canopy. (b) Photosynthetic active radiations PAR received at 6.5 m a.g.l. in the ND plot. (c) Cumulated precipitation P_{cum} measured over the ND (blue) and AD (red) plot. (d) Mean soil water content SW ± SD measured at -0.1 m depth from various soil probes in the ND (blue, *n*=3) and AD (red, *n*=5) plot.

Figure 2.: Seasonal variations of monthly *Q. pubescens* gas exchanges observed at O_3HP (June 2012 to 2013) under ND (blue) and AD (red) (mean ± SD). (a) Stomatal conductance to water vapour G_w. (b) Net photosynthetic assimilation P_n. (c) Measured branch isoprene emission rate ER. (d) Isoprene emission factor (I_s) calculated according to Guenther *et al.* (1993) using *in situ* ER *vs* $C_L \times C_T$ correlations, except in July where mean ER measured under enclosure conditions close to 1000 µmol m^{-2} s^{-1} and 30 °C was used. Differences between ND and AD using Mann-Whitney tests are denoted using lower case letters (a>b). Differences among months using Kruskal-wallis tests are denoted by asterisks (*: P<0.05; **: P<0.01; ***: P<0.001).

Figure 3: Calculated *vs* measured isoprene emission rates (ER) under ND (blue, *n*=267) and AD (red, *n*=138); from June 2012 to 2013, using (a) the MEGAN isoprene model (Guenther *et al.* 2006) with a wilting point value θw of 0.138 m^3 m^{-3} (Chen et Dudhia, 2001) and an isoprene emission fator (I_s) of 53 µgC g_{DM}^{-1} h^{-1} (Simpson *et al.*, 1999), and, (b) the isoprene emission algorithm *G*14 developped in this study; the linear regression relation is given together with the correlation coefficient R^2; dotted line is 1:1 line.

Figure 4.: Seasonal variations of the relative contribution on isoprene emission rates (ER) of (a) the environmental parameters used in *G*14 (the received incident PAR *L*, air temperature *T*, soil water content SW, soil temperature ST and precipitation *P*) whatever their frequencies considered in *G*14; and, of (b) the different frequencies in *G*14 (0, 7, 14, 21 days before the measurement), whatever the environmental parameters in *G*14.

Biogeosciences Discuss., doi:10.5194/bg-2017-17, 2017
Manuscript under review for journal Biogeosciences
Discussion started: 9 February 2017

Figure 5.: Present (2000-2010) to future (2090-2100) changes in the seasonal variations over the continental Mediterranean area obtained using RCP2.6 (left) and RCP8.5 (right) projections for (a) monthly precipitation (*P*, mm), air temperature (*T*, °C), soil temperature (ST, °C) and soil water content (SW, L_{H2O} L_{soil}^{-1}); (b) monthly ER absolute changes assessed using *G*14 (dER_{G14}) from March to October; (c) monthly ER relative changes assessed using *G*14 from March to October; (d) the relative impact of temperature (as the sum of *T* and ST, in blue) and water availability (as the sum of P and SW, in red) on ER_{G14} relative change; and, (e), the relative impact of different frequencies (instantaneous and cumulated over 7, 14 and 21 days) on ER_{G14} relative change. Inserted numbers are mean annual values.

Biogeosciences Discuss., doi:10.5194/bg-2017-17, 2017
Manuscript under review for journal Biogeosciences
Discussion started: 9 February 2017

Appendice 1: Calculation of isoprene emission rates ER (µgC g_{DW}^{-1} h^{-1}) using the *G*14 algorithm

Due to the large range of ER variations, emissions were considered as logER, where : logER=log[$ER_{(CN)}$]×*s* + *m* and *s* is the standard deviation of log de ER (xx), *m* is the mean of logER (xx), log[$ER_{(CN)}$] the central-normalised log10 of ER calculated as:

$$\log[ER_{(CN)}] = w_0 + w_{1,k} \times \tanh(N_1) + w_{2,k} \times \tanh(N_2) + w_{3,k} \times \tanh(N_3)$$

where $N_1 = w_{0,1} + \sum_{i=1}^{16}\sum_{j=1}^{16} w_{i,1} \times x_j$

$N_2 = w_{0,2} + \sum_{i=1}^{16}\sum_{j=1}^{16} w_{i,2} \times x_j$

$N_3 = w_{0,3} + \sum_{i=1}^{16}\sum_{j=1}^{16} w_{i,3} \times x_j$

Table A1. The optimised weights *w* as follows

w0	-1.29837907				
w0,1	-0,16226148	*w0,2*	2.90404784	*w0,3*	0.23868843
w1,1	0.07736039	*w1,2*	2.18450515	*w1,3*	-0.1283214
w2,1	0.04806346	*w2,2*	-0.0074737	*w2,3*	0.06711214
w3,1	-0.32907201	*w3,2*	0.31067189	*w3,3*	0.14496404
w4,1	0.54847219	*w4,2*	0.40895098	*w4,3*	-1.1895104
w5,1	-0.03820985	*w5,2*	0.27886813	*w5,3*	0.35561345
w6,1	0.34677986	*w6,2*	0.2906721	*w6,3*	-2.84020867
w7,1	-1.44104866	*w7,2*	-1.23651445	*w7,3*	4.30350692
w8,1	-0.63559865	*w8,2*	-0.63879809	*w8,3*	3.61172683
w9,1	0.81398482	*w9,2*	0.85053882	*w9,3*	0.46501183
w10,1	-2.01376339	*w10,2*	1.59664603	*w10,3*	-0.74513053
w11,1	1.61737626	*w11,2*	-1.68773125	*w11,3*	-2.29893094
w12,1	-0.57093409	*w12,2*	-0.76488022	*w12,3*	1.96571085
w13,1	0.78483127	*w13,2*	0.9786783	*w13,3*	-1.88733755
w14,1	0.05311514	w14,2	-0.88244467	w14,3	-1.90110521
w15,1	-0.47856411	w15,2	-0.88883049	w15,3	1.35713546
w16,1	0.39618491	*w16,2*	0.55564983	*w16,3*	-0.73830992
w1,k	-2.22601227	*w2,k*	-1.64346181	*w3,k*	-1.32117586

Biogeosciences Discuss., doi:10.5194/bg-2017-17, 2017
Manuscript under review for journal Biogeosciences
Discussion started: 9 February 2017

Table A2. The selected input regressors x_i as follows :

x_1	$L0$
x_2	L-1
x_3	$T0$
x_4	T-1
x_5	T_M-T_m
x_6	T-14
x_7	T-21
x_8	SW-1
x_9	SW-7
x_{10}	SW-14
x_{11}	SW-21
x_{12}	ST-7
x_{13}	ST-14
x_{14}	P-7
x_{15}	P-14
x_{16}	P-21

Biogeosciences Discuss., doi:10.5194/bg-2017-17, 2017
Manuscript under review for journal Biogeosciences
Discussion started: 9 February 2017

Biogeosciences Discussions Open Access EGU

Figure 1

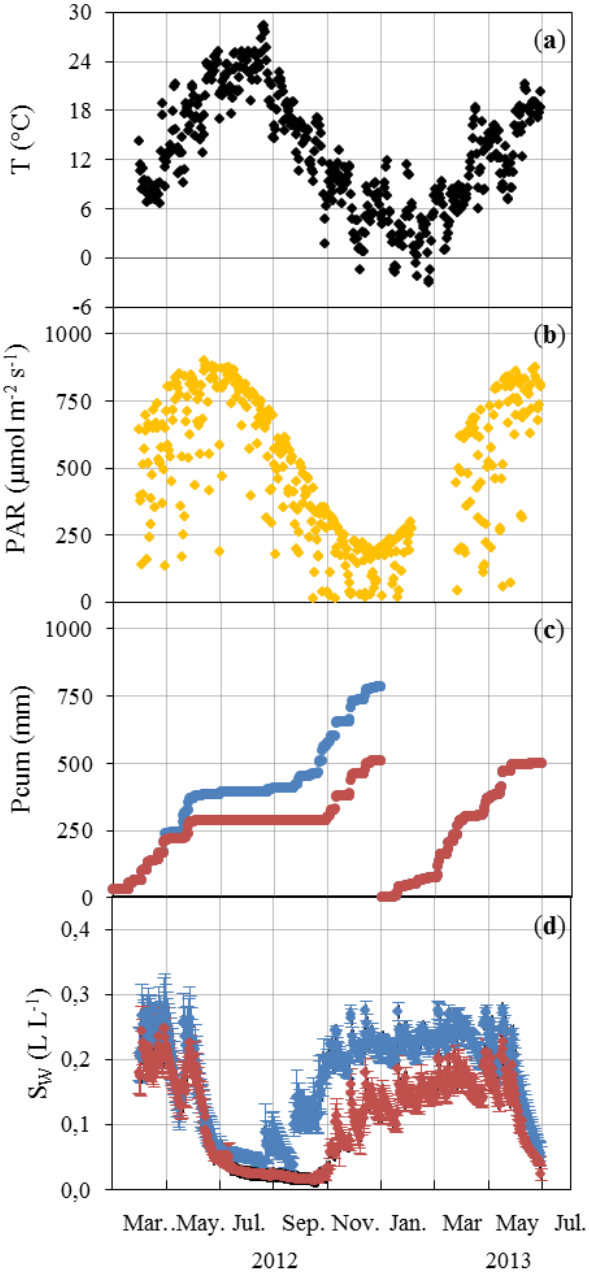

Biogeosciences Discuss., doi:10.5194/bg-2017-17, 2017
Manuscript under review for journal Biogeosciences
Discussion started: 9 February 2017

Biogeosciences Discussions
Open Access
EGU

Figure 2

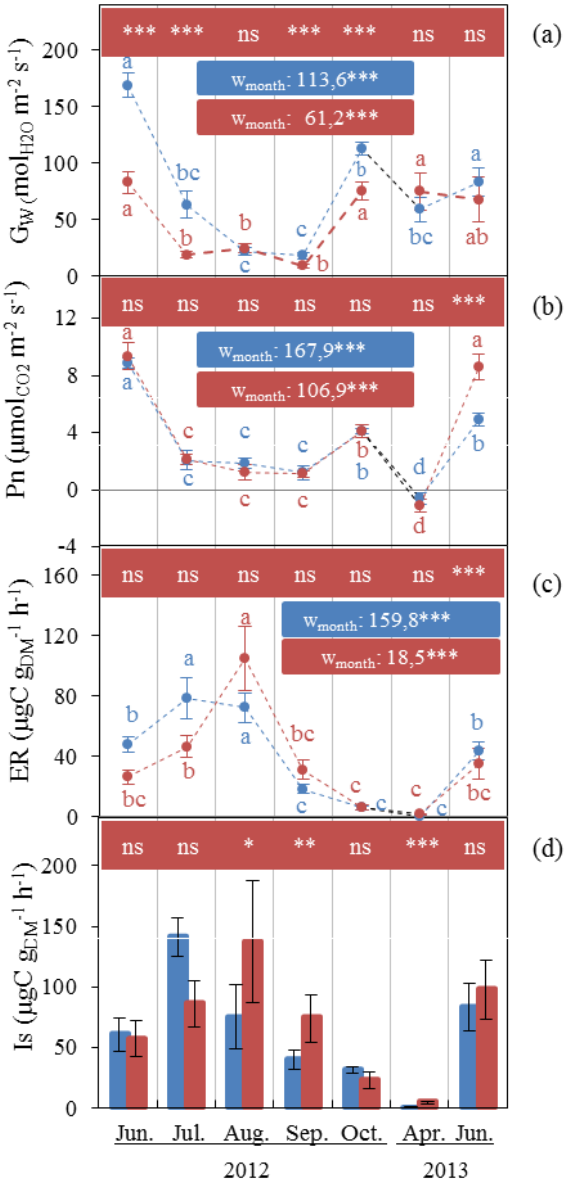

Biogeosciences Discuss., doi:10.5194/bg-2017-17, 2017
Manuscript under review for journal Biogeosciences
Discussion started: 9 February 2017

Figure 3

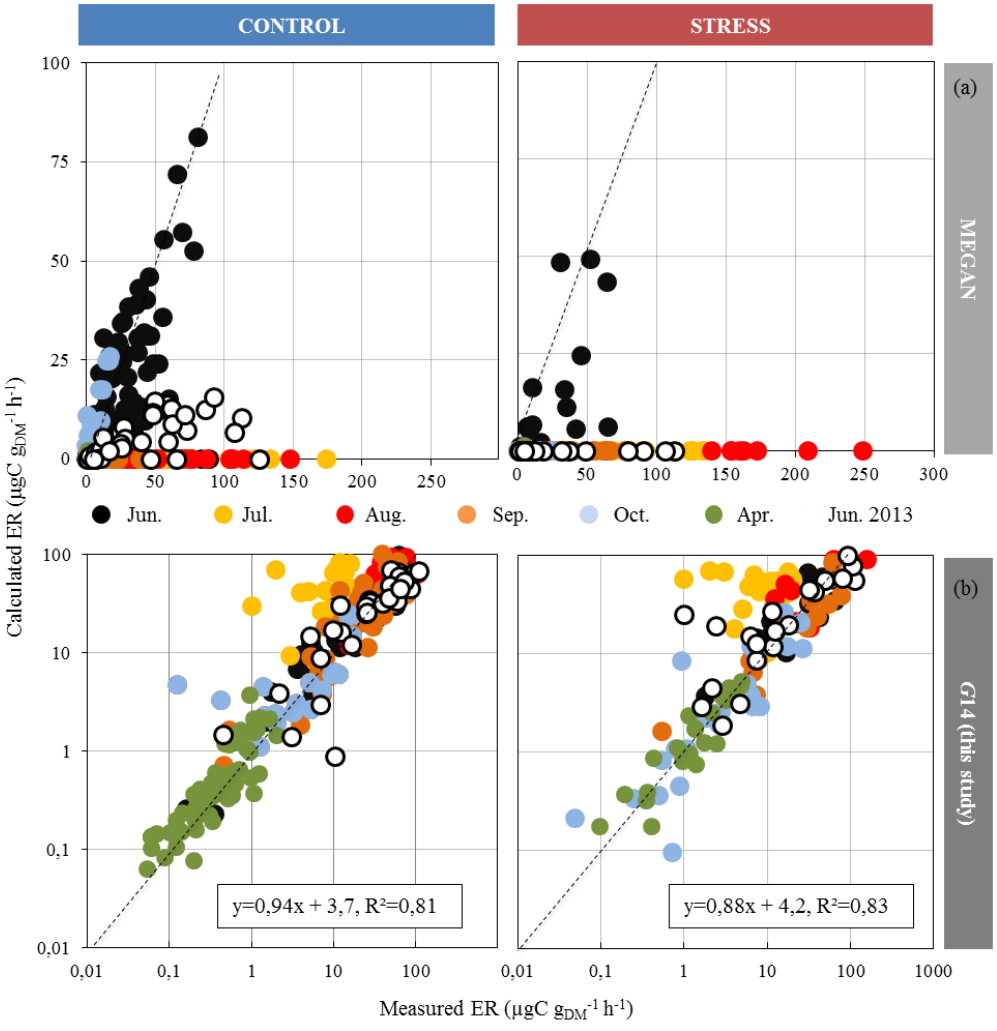

Biogeosciences Discuss., doi:10.5194/bg-2017-17, 2017
Manuscript under review for journal Biogeosciences
Discussion started: 9 February 2017

Figure 4

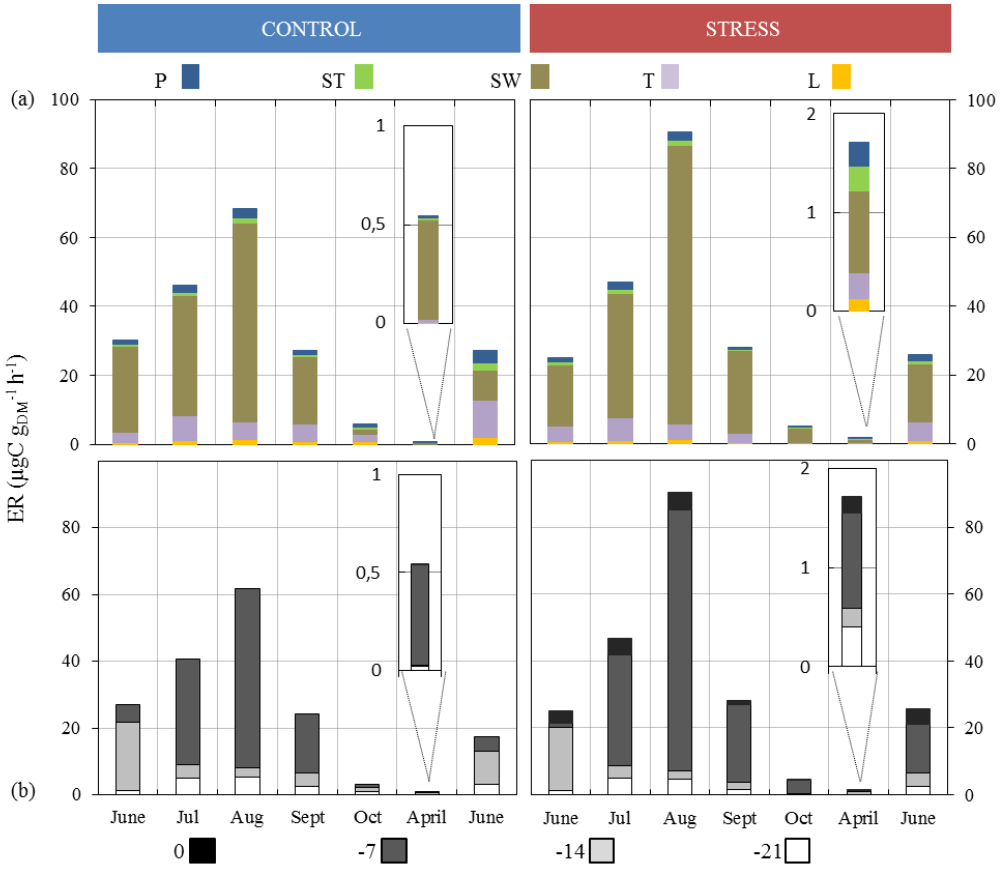

Biogeosciences Discuss., doi:10.5194/bg-2017-17, 2017
Manuscript under review for journal Biogeosciences
Discussion started: 9 February 2017

Figure 5